

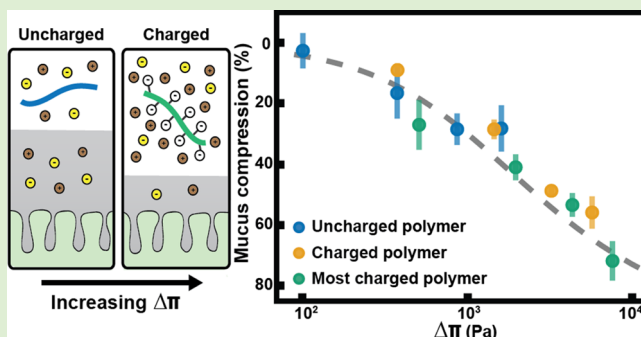
Food Polyelectrolytes Compress the Colonic Mucus Hydrogel by a Donnan Mechanism

Asher Preska Steinberg,[†] Zhen-Gang Wang,[†] and Rustem F. Ismagilov^{*,†,‡}

[†]Division of Chemistry and Chemical Engineering and [‡]Division of Biology and Biological Engineering, California Institute of Technology, 1200 E. California Blvd., Pasadena, California 91125, United States

S Supporting Information

ABSTRACT: Systems consisting of a polyelectrolyte solution in contact with a cross-linked polyelectrolyte network are ubiquitous (e.g., biofilms, drug-delivering hydrogels, and mammalian extracellular matrices), yet the underlying physics governing these interactions is not well understood. Here, we find that carboxymethyl cellulose, a polyelectrolyte commonly found in processed foods and associated with inflammation and obesity, compresses the colonic mucus hydrogel (a key regulator of host–microbe interactions and a protective barrier) in mice. The extent of this polyelectrolyte-induced compression is enhanced by the degree of polymer negative charge. Through animal experiments and numerical calculations, we find that this phenomenon can be described by a Donnan mechanism. Further, the observed behavior can be quantitatively described by a simple, one-parameter model. This work suggests that polymer charge should be considered when developing food products because of its potential role in modulating the protective properties of colonic mucus.



INTRODUCTION

In this work, we sought to understand how polymer charge influences polymer-driven mucus compression. The colonic mucus hydrogel is a critical barrier in the colon—it is the nexus of host–microbe interactions and it protects against microbial infiltration and physical insults.¹ This hydrogel, which lines the walls of the colon, is composed primarily of high-molecular-weight (MW) glycoproteins (~1.2 MDa) known as mucins and is held together by physical entanglements, chemical cross-links, and electrostatic interactions.^{2,3} Although the microbiology and chemical biology communities have exhaustively studied how microbes interact with this hydrogel and its biochemical composition,^{1,2,4,5} the underlying physics that governs the structural features of the colonic mucus hydrogel has only recently begun to be explored.⁶ In particular, it is vital to understand what influences the de-swelling or compression of this hydrogel because several studies have found correlations between changes in the mesh size and thickness of colonic mucus and changes in host health.^{7,8} Our recent work has found that neutral or uncharged polymers can compress the colonic mucus hydrogel by a mechanism that can be described using a simple, first-principles thermodynamics model based on Flory–Huggins solution theory.⁶ It was shown that for these uncharged polymers, the extent of polymer-induced mucus compression is increased by either increasing the polymer concentration or increasing the polymer MW at a given polymer concentration. However, the human diet contains many charged polymers (i.e., polyelectrolytes), which are predominately negatively charged.^{9,10}

One polyelectrolyte that is commonly placed in food and is “generally regarded as safe” (GRAS) by the U.S. Food & Drug Administration (FDA) is carboxymethyl cellulose (CMC).¹¹ This polyelectrolyte is a cellulose derivative that has a negative charge in the gut due to carboxymethyl groups attached to some of its monomer units.¹² Interestingly, although many charged versions of CMC exist, the FDA allows only up to a degree of substitution (DS) of 9 charged groups per 10 monomers (abbreviated as “DS 0.9”). There is no existing literature explaining how changing the charge of these polymers affects the design of food products. CMC is added to processed foods because of its ability to enhance the viscosity of food and to stabilize emulsions by slowing droplet coalescence,^{9,13} which leads to it often being mistakenly called an “emulsifier” even though it is not a surfactant but a high-MW polyelectrolyte. Recent biological studies found that feeding mice CMC resulted in low-grade inflammation and obesity. CMC feeding was also correlated with a thin mucus layer that allowed for microbial encroachment upon the host.^{14,15} In addition, it has been shown that acute exposure to CMC (by direct injection into the small intestine) can alter the structure of the small intestine mucus layer in rats.¹⁶ However, mechanistic understanding of these effects is lacking; it is unclear if, in vivo, colonic mucus is thinner because it is disrupted or compressed. We hypothesize that the thin colonic

Received: March 29, 2019

Revised: May 23, 2019

mucus layer in mice fed CMC was the result of mucus compression.

Many studies have covered the physical chemistry of polyelectrolyte solutions,^{17,18} polyelectrolyte hydrogels,^{19,20} complex coacervation between oppositely charged polyelectrolytes,^{21,22} and complexation between polyelectrolytes with oppositely charged objects.^{23,24} In contrast, the interactions between systems composed of polyelectrolyte solutions and polyelectrolyte gels remain vastly understudied,²⁵ both experimentally and theoretically. Here, we seek to untangle the physical interactions between colonic mucus (a biological polyelectrolyte gel) and CMC (a polyelectrolyte).

MATERIALS AND METHODS

Details of Animals Used. All mice were 2–6 months old, male or female specific-pathogen-free (SPF) C57BL/6 mice (RRID: IM-SR_JAX:000664). In our previous study, we did not observe any differences in mucus compression related to age (in the same age range as this study) or gender.⁶ We justified the use of both male and female mice because an experimental study found that ~3-month-old C57BL/6 mice had similar mucus thickness and morphology regardless of sex.²⁶ We justified the use of a range of ages of mice because, although it has been reported that 19-month-old C57BL/6 mice had thinner colonic mucus compared to 2.5–3-month-old C57BL/6 mice, 19 months old is well outside the age range of this study.^{26,27} Mice used in ex vivo experiments in Figures 2–4 and Figure S1 were maintained on a solid chow diet (PicoLab Rodent Diet 20) and were given food and water ad libitum. Mice used in experiments in Figure 1 were maintained on a chow diet until the day of the experiment. Starting 23 h before euthanization, these mice were restricted (no chow or water) to a solution of 1% w/v carboxymethyl cellulose (carboxymethylcellulose sodium, USP grade, medium viscosity, PN: C9481-500G) with 5% w/v sucrose (USP grade, PN: S3929) in water or a solution of 1% v/v Tween (polysorbate 80, food grade, Sigma-Aldrich, PN: W291706) with 5% sucrose in water. For these 23 h, mice were kept on mesh-bottom cages to prevent re-ingestion of chow-derived polymeric contents from fecal matter. All mice were obtained from Jackson Labs (The Jackson Laboratory, Bar Harbor, ME, USA) and were then housed at Caltech's animal facility. All animal experiments were approved by the California Institute of Technology (Caltech) Institutional Animal Care and Use Committee (IACUC; protocol no. 1691) and the U.S. Army's Animal Care and Use Review Office (ACURO; protocol no. 70905-LS-MUR.03). Mice were euthanized via CO₂ inhalation as approved by the Caltech IACUC in accordance with the American Veterinary Medical Association Guidelines on Euthanasia.²⁸

Details of Microscopy. Images were acquired by taking z-stacks on a Zeiss LSM 880 upright confocal microscope using confocal fluorescence to image particles (488 nm excitation/505–736 nm band pass filter), confocal reflectance to image the epithelium (561 nm excitation/505–736 nm band pass filter), bright field for the epithelium and particles, or two photon for the FC oil layer and epithelium (700 or 750 nm excitation/650–758 nm band pass filter).

Imaging of Samples Using “FC Oil Approach”. Sample preparation and imaging were carried out as described previously in ref 6 (in ref 6, see Supporting Information Materials and Methods, section “Imaging of Unwashed Tissue”).

Imaging of Samples Using “Microparticle Approach”. Sample preparation and imaging were carried out as described previously in ref 6 (in ref 6, see Supporting Information Materials and Methods, sections “Imaging of Washed Mucus Hydrogel” and “Thickness Measurements of Washed Mucus Hydrogel”). The protocol was modified such that the fluorescent 1 μ m diameter polystyrene beads coated with poly(ethylene glycol) (PEG) with a molecular weight (MW) of 5 kDa were used as the microparticles (created as described in ref 29). These were imaged using fluorescence in addition to confocal reflectance (488 nm excitation/505–736 nm band pass filter). For the thickness measurements obtained using the micro-

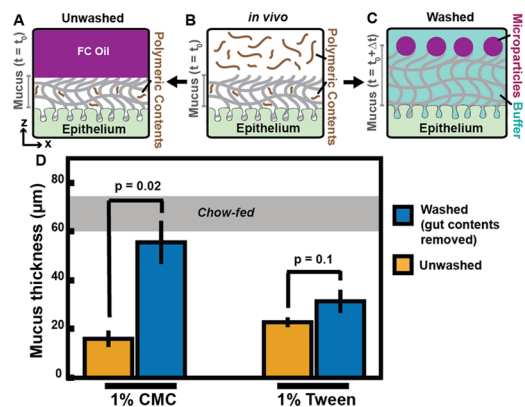


Figure 1. Carboxymethyl cellulose (CMC) compresses the colonic mucus hydrogel in vivo. (A) Cartoon side view depicting the fluorocarbon (FC) oil imaging setup, which retains polymeric contents in contact with colonic mucus, prevents dehydration, and maintains mucus at a similar thickness (t) to that of initial in vivo thickness (t_0). (B) In vivo, the mucus hydrogel is in contact with polymeric contents that can compress mucus. (C) Cartoon side view depicting the microparticle imaging setup in which polymeric contents are washed away with buffer and particles with a diameter (d) greater than the mucus mesh size (ξ) are used to measure mucus thickness. The mucus thickness increases (Δt) from in vivo when “compressive” polymers are absent. (D) Mucus thickness measurements from mice fed either a solution of 1% CMC + 5% sucrose (1% CMC) or a solution of 1% Tween + 5% sucrose (1% Tween) for 23 h. The mucus thickness is plotted on the vertical axis (in μ m) for different groups of mice. Measurements using the microparticle approach (“washed (gut contents removed)”) are in blue; thickness measurements obtained using the FC oil approach (“unwashed”) are in orange (see ref 6 for details and validation of approach). Thickness measurements represent the average thickness measured on explants from individual mice. Error bars are the standard error of the mean (SEM) where n = the number of mice. All groups contained at least three mice. P values were obtained using Welch’s t -test. The gray bar across the figure indicates mucus thickness measured for chow-fed mice using the FC oil approach from our previous study,⁶ where we measured $t = 67 \pm 7 \mu\text{m}$ (mean \pm SEM). The bottom of the bar is $t = 60 \mu\text{m}$, and the top of the bar is $t = 74 \mu\text{m}$.

particle approach shown in Figure 1, determination of the mucus thickness was done in the same way as the FC oil approach.

Compression Measurements. Compression measurements were carried out as described in ref 6 (in ref 6, see Supporting Information Materials and Methods, section “Quantifying Polymer-induced Compression of Washed Mucus Hydrogel”). In this work, we define “% compression” as % compression = $[\Delta t/t_0] \times 100\%$, where t_0 is the initial mucus thickness, and $\Delta t = t_0 - t_f$ where t_f is the final mucus thickness. We modified the protocol such that each compression measurement in this work represents the mean of compression measurements taken on colonic explants from three separate mice. The compression value from each individual explant is the average of compression measurements in five different positions on that explant. The error bars are the standard error of the mean with $n = 3$. For measurements done with 1 \times phosphate-buffered saline (PBS), we diluted 10 \times PBS (Corning 10 \times PBS, pH 7.4 ± 0.1 , without calcium and magnesium, RNase-/DNase- and protease-free, product no. 46-013-CM) 10-fold with Milli-Q water. In the compression experiments in Figure 4 with polymers in 10 \times PBS, the tissue was incubated with microparticles in 1 \times PBS for ~ 1 h before placing on the polymers in 10 \times PBS. The final thickness was then measured after 10 min. This was done to prevent prolonged exposure (1 h or longer) to 10 \times PBS (which after long times could cause tissue deterioration due to the salt imbalance) while the microparticles sedimented down on the top of the mucus hydrogel.

Polymers Used for Compression Measurements. We used carboxymethyl cellulose (CMC) with a degree of substitution (DS) of 7 charged monomers per 10 monomers (DS 0.7) (Sigma-Aldrich, PN: 419311), CMC DS 0.9 (Sigma-Aldrich, PN: 419303), and hydroxyethyl cellulose (HEC) (Sigma, PN: 308633).

Gel Permeation Chromatography (GPC) of Polymers. GPC was used to measure the MW and hydrodynamic radii (R_h). This was used to confirm that CMC used in the mouse-feeding experiments in Figure 1, and CMC and HEC used in all other figures were approximately the same MW and R_h (measurements shown in Figure S3 and Table S1). GPC measurements were conducted as described in ref 29. CMC derivatives were analyzed using a refractive index increment (dn/dc) of $\frac{dn}{dc} = 0.163$.³⁰ HEC was analyzed using $\frac{dn}{dc} = 0.150$.³¹

Curve Fitting in Figure 3. For the curve fitting presented in Figure 3, we used the “`scipy.optimize.curve_fit`” function in Python 3.6.4, which is included as a supplemental file to the manuscript.

RESULTS AND DISCUSSION

Carboxymethyl Cellulose (CMC) Compresses Mucus Reversibly in Vivo. We first sought to test two hypothesis: (1) the colonic mucus hydrogel is thin when mice are fed CMC because the mucus hydrogel is compressed; (2) the mechanism by which CMC interacts with mucus is different than that of an emulsifier—polysorbate 80 (Tween 80)—because of the differences in their physicochemical properties (CMC is a high-MW polyelectrolyte, whereas Tween is a low-MW, nonionic surfactant).

To test these two hypotheses, we devised a simple experiment in which we fed one group of SPF mice a solution of 1% w/v CMC and another group 1% w/v Tween 80 for 23 h, and then measured the thickness of the mucus hydrogel. We justified the removal of the standard chow diet because our previous work with different dietary polymers suggested that the components of chow do not contribute to mucus compression in SPF mice.⁶ We tested this in ref 6 by measuring mucus compression on colonic explants using polymers in buffer and comparing it to compression induced by the same polymers prepared in extracted luminal fluid from chow-fed SPF mice. We found similar amounts of compression. Additional evidence supporting this in ref 6 was that adding the luminal fluid from chow-fed SPF mice to colonic explants did not induce mucus compression and that, for chow-fed SPF mice, the mucus thickness on explants remained the same when luminal contents were removed. In this work, for our experiment to test the differences between feeding 1% w/v CMC and 1% w/v Tween 80, we first measured the thickness of the mucus hydrogel using our fluorocarbon (FC) oil approach (Figure 1A,B; see ref 6 for further details). Briefly, this method allows us to avoid washing colonic explants with buffer (which could cause the loss of polymeric contents that are in contact with the mucus hydrogel), and it eliminates the use of a fixative (which could alter mucus structure). Instead, we remove luminal contents with FC-40 oil, which is immiscible with and denser than water, and coat the explant with FC-40 oil, which sits on the top of mucus. The FC oil approach has the further advantage of preventing dehydration of the mucus layer, allowing us to measure the extent of compression as it would be in vivo. The thickness is then obtained by measuring the difference in the position of the epithelial cells under mucus (identified using bright-field and confocal reflectance) and the position of the FC oil–hydrogel interface (identified using

confocal reflectance). We found that both the CMC and Tween 80 groups had a thin mucus layer (Figure 1D, gold bars) compared with previous thickness (t) measurements we had done with groups of mice fed a standard chow diet, where we measured $t = 67 \pm 7 \mu\text{m}$ (ref 6; Figure 1D, gray bar).

The FC oil approach allows us to measure the mucus thickness in an environment that approximates the “native state” of the adherent, colonic mucus hydrogel when it is in contact with in vivo gut contents (see ref 6 for further details and validation of this approach). However, we wanted to test whether the mucus was thin because it was disrupted or whether it was compressed. We therefore used a different tissue preparation approach that allowed us to measure the mucus thickness after washing out the in vivo gut contents (including polymers and other molecules that could disrupt or compress mucus). We took two more groups of mice and fed them with the same solutions, but this time, before imaging, we washed the tissue with phosphate-buffered saline (PBS) to remove any colonic polymeric contents that could compress mucus. We then quantified the mucus thickness using the “microparticle approach” (Figure 1B,C; Materials and Methods). This and similar approaches have been used previously to quantify the thickness of the adherent, inner colonic mucus layer ex vivo.^{6,7,32} Briefly, in the microparticle approach, after removing all gut contents, a solution of microparticles (in PBS) with a diameter (d) larger than the mucus mesh size (ξ) is allowed to sediment down on the top of the mucus hydrogel. These microparticles were coated with polyethylene glycol (PEG), as PEG coating has been previously shown to reduce the mucoadhesivity of particles.³³ Because $d > \xi$, the microparticles are excluded from the hydrogel (which we confirmed in our previous work⁶), and we can determine the thickness by measuring the difference in the position of the epithelium (using confocal reflectance and bright-field) and the position of the microparticles (using fluorescence). Using the microparticle approach, we observed that the mucus layer was substantially thicker in the CMC group than in the Tween group (Figure 1D, blue bars). Furthermore, we observed that the mucus in the “washed” CMC-fed group was substantially thicker than the mucus in the “unwashed” CMC-fed group. The reversibility of the effect suggests that the mucus hydrogel in CMC-fed groups is compressed in vivo, springing back when “compressive” polymeric contents are washed out with buffer. The reversibility also suggests that the alternative hypothesis, that the polymer itself degrades mucus, is incorrect; degradation would likely disrupt the integrity of the mucus hydrogel and not allow it to recover its thickness. Another potential factor is that the gut microbiota has been shown to degrade colonic mucus in different contexts.⁴ However, because the mucus thickness in the “washed” CMC-fed group agreed with our previous measurements of the inner mucus layer in chow-fed mice (i.e., the “normal” mucus thickness in healthy, SPF mice), it suggests that the colonic mucus hydrogel is not degraded by the gut microbiota over the course of our experiments. For the Tween-fed groups, our data showed that both the washed and unwashed Tween-fed groups had thinner mucus compared with the washed CMC-fed group (Figure 1D) and our previous measurements of mucus in chow-fed mice. Because the “normal” thickness of the inner mucus layer could not be recovered, it suggests that in the Tween-fed groups, mucus was irreversibly “thinned”. In total, these experiments suggest that not only does CMC compress the colonic mucus hydrogel

reversibly *in vivo*, but the physical mechanism by which it interacts with mucus is different than that of Tween. This observation was unexpected because polyelectrolytes and emulsifiers have been considered to be similar in previous gut studies.^{14,15,34} We therefore sought to understand the mechanism by which CMC compresses the colonic mucus hydrogel.

Carboxymethyl Cellulose (CMC) Degree of Charge Increases Extent of Mucus Compression. We next sought to understand the mechanism by which CMC compresses the colonic mucus hydrogel. Here, we aimed to test whether modulating the amount of charge on CMC could influence the extent of mucus compression. We first tested if CMC compressed mucus *ex vivo*. We used our microparticle approach to measure the initial thickness of mucus (t_0) on a colonic explant, then placed the explant in a solution of 1% w/v CMC DS 0.7 (Figure 2A), waited 10 min, and measured the

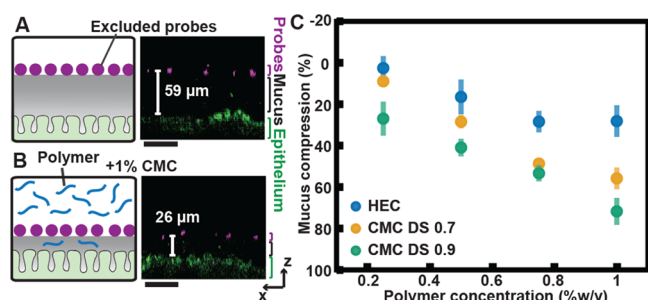


Figure 2. Negatively charged CMC compresses mucus *ex vivo* more than uncharged polymers. (A, B) Cartoons (left) and images (right) in the side view show the 1 μm diameter particles (purple) sitting on the top of the mucus (A) before and (B) after the addition of 1% w/v CMC solution. The epithelium is shown in green. (C) Plot of mucus compression (where % compression = $[\Delta t/t_0] \times 100\%$, further details in Materials and Methods) as a function of polymer concentration (% w/v). Each data point represents the average of compression measured on three independent replicates (three explants from different mice), where the compression from an individual replicate is the average of five compression measurements at lateral positions on the explant. Error bars are SEM with $n = 3$. HEC = hydroxyethyl cellulose, CMC DS 0.7 = CMC with a degree of substitution of 7 negatively charged groups per 10 monomers, and CMC DS 0.9 = CMC with a degree of substitution of 9 negatively charged groups per 10 monomers. Images shown in side views were processed as described in ref 6 and Figure S1.

thickness (t_f) (Figure 2B). We found that CMC compressed the mucus hydrogel (Figure 2A–B) and that the extent of compression remained constant over the course of 30 min (Figure S2), suggesting that the system had reached a steady state. Similarly, in our previous study, we found compression by an uncharged polymer (polyethylene glycol) was constant over the course of 60 min.⁶ Additionally, for CMC, the compression was reversible—by washing out the CMC solution with buffer, the hydrogel returned to its initial thickness (Figure S2). As with the *in vivo* experiments, the *ex vivo* reversibility suggests that the observed phenomenon is a form of compression as opposed to degradation of the mucus hydrogel because in the latter case, the hydrogel would likely be unable to recover its initial thickness.

To understand how negative polymer charge affects the extent of compression, we next compared how mucus compression differed as a function of polymer concentration

for CMC DS 0.7, CMC DS 0.9 (a derivative of CMC that is more charged than CMC DS 0.7), and hydroxyethyl cellulose (HEC, a cellulose derivative with the same chemical backbone but no charge). Each polymer was added in a range of concentrations that are approved by the FDA for addition to food¹¹ and commonly used in processed foods.⁹

Generally, the extent of mucus compression increased with increased polymer concentration for all three polymers (Figure 2C). We found that at most polymer concentrations, the more highly negatively charged polymer (CMC DS 0.9) induced the most compression (Figure 2C). In contrast, the neutral polymer (HEC) generally induced the least compression at any given polymer concentration (Figure 2C). These data suggest that, generally, the negative charge of the polymer increases the extent of mucus compression.

Mucus Compression due to Charged Polymers Is Consistent with a Donnan Mechanism.

We knew from previous studies with the colonic mucus hydrogel (specifically, the stratified, cross-linked mucus hydrogel, which is firmly adhered to the epithelium) and the periciliary brush that the polymer-induced compression of biological polymer networks can be driven by the differences in osmotic pressure between the external polymer solution and the solution phase internal to the cross-linked polymer network.^{6,35} In such scenarios, the osmotic pressure difference ($\Delta\Pi$) drives the flux of water out of the polymer network, causing the network to shrink or compress; the equilibrium gel volume is determined by the balance between $\Delta\Pi$ on the one hand and the mixing pressure (due to the change in free energy from mixing the gel with solvent and free polymer) and the pressure associated with the elastic deformation of the network chains (i.e., elastic contributions) on the other hand.³⁶ An alternative, equivalent conceptualization is that at equilibrium, the osmotic pressure of the external solution is equal to the following contributions from the hydrogel phase: the osmotic pressure of the solution internal to the hydrogel, the mixing pressure, and elastic contributions. It has been well established that polyelectrolyte solutions and gels can also preferentially partition ions between phases,^{19,37,38} causing an increase in the osmotic pressure of the polyelectrolyte phase compared with that of the external solution phase with which it is in contact. This is what is known as Donnan partitioning or a Donnan mechanism. Given that both CMC and the adherent, cross-linked colonic mucus hydrogel itself are both negatively charged, we therefore hypothesized that the theory of Donnan partitioning could be used to explain the enhancement of mucus compression we observed with increased polymer charge. In previous studies with synthetic hydrogels, polymer-induced compression has been experimentally quantified by visualizing changes in hydrogel volume, and an explanation of these results has been offered using well-established theoretical frameworks such as the Flory–Huggins theory and the Flory–Rehner theory.^{39–45} We therefore sought to use a similar methodology to understand if polyelectrolytes compress the colonic mucus hydrogel by a Donnan mechanism.

Before testing our hypothesis with numerical calculations, we first wanted to understand if mucus exhibits Donnan partitioning in a simple scenario when the colonic mucus hydrogel is placed in a buffered solution without CMC. First, we write down the condition of electroneutrality for both the external buffer solution (ext) and inside mucus (int)^{46,47}

$$c_+^{\text{ext}} = c_-^{\text{ext}} = c_0 \quad (1)$$

$$c_+^{\text{int}} = c_-^{\text{int}} + m \quad (2)$$

where c_+ denotes the molar concentration of mobile cations, c_- is the molar concentration of mobile anions, c_0 is the concentration of monovalent salt, and m is the molar concentration of charges on mucus (this analysis assumes that the polyelectrolyte counterions are the same as the salt cations). In this case, the cation for CMC is Na^+ , and the cation in the buffer is predominantly Na^+ , as explained below. Invoking the equality of electrochemical potential for the mobile ions and combining eqs 1 and 2 give us

$$\frac{c_+^{\text{int}}}{c_0} = \frac{m}{2c_0} + \sqrt{\left(\frac{m}{2c_0}\right)^2 + 1} \quad (3)$$

Equation 3 gives the fractional increase of positively charged ions inside the mucus hydrogel due to Donnan partitioning. In our experiments, we use PBS as the buffer, which by the molar concentration is $\sim 90\%$ NaCl. Therefore, we approximated the ionic strength to be equal to the molar concentration of NaCl: $c_0 = 137$ mM. We can estimate the molar concentration of negative charges on mucus by estimating the volume fraction of mucus (ϕ_m) to be $\phi_m \sim 1\%$ (this is consistent with results from the literature: refs 6, 48–50), which, combined with the amount of charged groups per mucin,⁴⁷ yields $m \sim 5$ mM. This yields $\frac{c_+^{\text{int}}}{c_0} \cong 1.02$. We can therefore assume that any differential salt partitioning by the colonic mucus hydrogel itself at physiological ionic strengths is negligible.

Our previous numerical results for polymer-induced mucus compression⁶ suggested that an uncharged polymer of a similar MW, and the radius of gyration (R_g) to the polymers used in this study (PEG 200 kDa with $R_g \sim 22$ nm) is mostly excluded from mucus—the ratio of polymers inside mucus to the polymers in the external solution was at most ~ 0.3 and approached 0 as the polymer concentration increased. The HEC and CMC used in this study are slightly larger than PEG 200 kDa; the measured hydrodynamic radius (R_h) of HEC and CMC from our gel permeation chromatography (GPC) measurements (see Table S1 and Figure S3) is $R_h \sim 20$ nm, which we can use in conjunction with the Kirkwood–Riseman relation⁵¹ to estimate $R_g \sim 30$ nm. In addition, the charged polymers should experience electrostatic repulsions with the mucin strands (which also have some negative charge). We would therefore expect that HEC and CMC should be even more excluded from mucus than PEG 200 kDa. If we then take as a second simplifying assumption that the polymer is completely excluded from mucus, we can write down $\Delta\Pi$ (in units of Pa) as¹⁷

$$\Delta\Pi = \Delta\Pi_{\text{ion}} + \Pi_{\text{pol}} \quad (4)$$

where $\Delta\Pi_{\text{ion}}$ is due to Donnan partitioning of the small ions between the external polyelectrolyte solution and the mucus network and can be written as (see Supporting Information for derivation)

$$\frac{\Delta\Pi_{\text{ion}}}{RT} = 2c_0 + p - 2\sqrt{c_0(c_0 + p)} \quad (5)$$

where R is the gas constant, T is the temperature (in kelvin), and p is the molar concentration of charges from the charged polymer (which we know because the number of charges per monomer is given by the manufacturer and we determined the polymer MW by GPC; Table S1 and Figure S3). The polymer

osmotic pressure (Π_{pol}) for an uncharged polymer can be written as⁵²

$$\frac{\Pi_{\text{pol}}}{RT} = \frac{c_p}{MW} \left(1 + \left(\frac{c_p}{c_p^*} \right)^{1.3} \right) \quad (6)$$

where c_p is the polymer concentration (in kg/m^3), MW is the polymer molecular weight (in Da), and c_p^* is the polymer overlap concentration (in kg/m^3), which can be estimated as⁵²

$$c_p^* = \frac{MW}{\frac{4\pi}{3} N_{\text{avo}} R_g^3} \quad (7)$$

where N_{avo} is the Avogadro number and R_g is the polymer radius of gyration (in m). The polymer MW, based on our GPC measurements, is ~ 150 kDa (Table S1 and Figure S3). We can use this along with the polymer R_g and eq 7 to calculate $c_p^* \approx 1.9$ kg/m^3 . This justifies the use of eq 6 for the polymer osmotic pressure instead of the osmotic pressure for a dilute polymer solution (which would simply be the first term of eq 6) because the polymer concentrations we test in this study all exceed the polymer overlap concentration, meriting the inclusion of the second term in eq 6, which accounts for the behavior above overlap concentration. Using eq 4–7, we estimated $\Delta\Pi$ for both the neutral and charged polymers used in Figure 2C. For the charged polymers, the ionic contribution to the osmotic pressure (eq 5) is substantially greater than the polymer contribution (eq 6) at all polymer concentrations, suggesting the Donnan mechanism contributes more to $\Delta\Pi$ (see Figure S4). We plotted the extent of mucus compression against $\Delta\Pi$ in Figure 3B. We found that the extent of compression generally increases with $\Delta\Pi$. Furthermore, the relationship between mucus compression and $\Delta\Pi$ has a similar functional form to the classical stress–elongation relation for uniaxial deformations from the affine network model, which

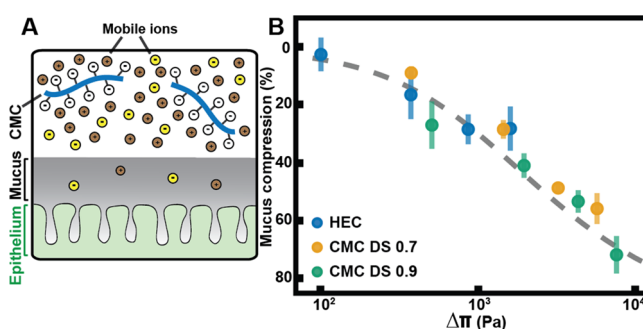


Figure 3. Extent of mucus compression plotted against the difference in osmotic pressure ($\Delta\Pi$) due to the added polymer. (A) Cartoon depicting the theoretical picture of Donnan partitioning by charged polymers (labeled “CMC”). Mobile ions are preferentially partitioned outside of mucus by the charged polymers. (B) Extent of mucus compression plotted against the theoretical calculation of $\Delta\Pi$. Compression values are the same experimental data as Figure 2C. The dashed line is a fit to the classical stress–elongation relation, where $\Delta\Pi = G\left(\lambda - \frac{1}{\lambda^2}\right)$ and $\lambda = 1 - \frac{\text{mucus compression}}{100}$. G (the compression modulus) was used as a free parameter, and in the fit, $G = 749$ Pa. HEC = hydroxyethyl cellulose, CMC DS 0.7 = carboxymethyl cellulose with a degree of substitution of 7 charged monomers per 10 monomers, and CMC DS 0.9 = carboxymethyl cellulose with a degree of substitution of 9 charged monomers per 10 monomers.

has been used previously to describe the compression of hydrogels composed of biopolymers^{53,54} and synthetic polymers^{55,56} and can be written as⁵²

$$\sigma_{\text{eng}} = -G\left(\lambda - \frac{1}{\lambda^2}\right) \quad (8)$$

where σ_{eng} is the engineering stress or the applied stress on the network (which, in this case, is $\Delta\Pi$), G is the compression modulus of the network (in Pa), and λ is the deformation factor, which is related to % mucus compression through: $\lambda = 1 - \frac{\% \text{ mucus compression}}{100}$. The negative sign is included because the stress is compressive. A fit to eq 8 is plotted as the dashed line in Figure 3B. We take G as the one free parameter in this fit, which yields ~ 750 Pa. We are not aware of directly measured values for G for colonic mucus. However, this fitted value is of the same order of magnitude as that estimated using available literature data (see Supporting Information for details). Ultimately, it is both the collapse of the mucus compression data largely onto a single curve in Figure 3B and the functional form of this curve that suggest that the mucus hydrogel is undergoing a form of uniaxial deformation induced by $\Delta\Pi$.

Overall, this analysis, which relies on well-established theoretical frameworks,^{17,19,46,52} suggests that it is the difference in the osmotic pressure between the external polyelectrolyte solution phase and the solution phase within the mucus hydrogel, which drives the compression of mucus by CMC. It further suggests that the difference in the osmotic pressure and the concomitant compression is increased for polyelectrolytes via a Donnan mechanism.

Increasing Ionic Strength Decreases Mucus Compression by Polyelectrolytes. Because our data in Figure 3B suggested that the increase in the amount of compression we see for polyelectrolytes is due to a Donnan mechanism, we devised a simple set of experiments to test this hypothesis further. It is known that the amount of Donnan partitioning decreases with increasing salt concentration (this can be seen by inspection of eqs 3 and 5). We therefore formulated two hypotheses: (i) Polyelectrolyte-induced compression will be reduced by high ionic strength because $\Delta\Pi_{\text{ion}}$ is reduced (see Figure 4A,B). (ii) For uncharged polymers, the amount of compression will remain the same when the ionic strength is increased because there is no contribution from $\Delta\Pi_{\text{ion}}$ at any ionic strength.

We expect the most significant increase in compression due to Donnan partitioning to occur in the 1% w/v CMC DS 0.9 solution, which has the highest molar concentration of charges. By solving eq 5, we find that for 1% CMC DS 0.9 in a 1× PBS solution ($c_0 \sim 0.137$ M), $\Pi_{\text{ion}} \sim 6000$ Pa. If we increase the ionic strength 10-fold to $c_0 \sim 1.37$ M by using a 10× PBS solution, this decreases to $\Pi_{\text{ion}} \sim 700$ Pa. We would therefore anticipate that such an increase in the ionic strength would reduce the compression caused by 1% CMC DS 0.9.

We then tested our hypothesis experimentally by comparing the measured compression for 1% CMC DS 0.9 in 1× PBS to that of 1% CMC DS 0.9 in 10× PBS and found, consistent with our first hypothesis, that there was more compression in the 1× PBS solution (Figure 4C). We then tested if the high ionic strength treatment (10× PBS) affected the amount of compression for 1% HEC (an uncharged polymer) and found, consistent with our second hypothesis, that compression was the same for 1× and 10× PBS treatments (Figure 4C). As a

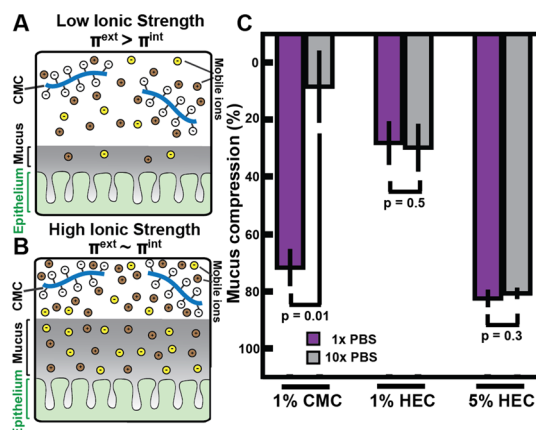


Figure 4. Increasing the ionic strength decreases the extent of polyelectrolyte-induced mucus compression, consistent with a Donnan mechanism. (A, B) Schematic depicting the decrease in polyelectrolyte-induced mucus compression in buffer solutions with high ionic strength: (A) When ionic strength is low, there is a greater difference in the concentrations of mobile ions in the external phase (the polymer solution) and internal phase (the mucus gel). Subsequently, there is a greater difference in the external osmotic pressure (Π^{ext}) compared to the internal osmotic pressure (Π^{int}). (B) When ionic strength is high, polyelectrolytes still partition mobile ions, but there is a smaller difference in the concentrations of mobile ions between the polymer solution and the mucus hydrogel. Therefore, there is a smaller difference in Π^{ext} compared to Π^{int} . (C) Extent of mucus compression as determined via the microparticle imaging approach. Each bar represents the mean of compression measurements from three biological replicates (each replicate is a colonic explant from a mouse). The compression value from each individual replicate is the average of compression measurements acquired at five different lateral positions on that explant. Error bars are SEM with $n = 3$. P values were computed using Welch's t -test; 1% CMC = 1% w/v carboxymethyl cellulose with DS 0.9, 1% HEC = 1% w/v hydroxyethyl cellulose, 5% HEC = 5% w/v hydroxyethyl cellulose, 10× PBS = phosphate-buffered saline at 10-fold its normal concentration, and 1× PBS = phosphate-buffered saline at its normal concentration.

control, to ensure that the high ionic strength was not disrupting the integrity of the mucus hydrogel and eliminating its compressibility, we tested for compression on colonic explants with 10× PBS at a high concentration of HEC (5% w/v). We found the mucus compressed to equal amounts in both 1× and 10× PBS treatments (Figure 4C), suggesting that high ionic strength does not disrupt the integrity of the colonic mucus hydrogel.

Overall, these data suggest that the increase in mucus compression observed in response to polyelectrolytes, compared with uncharged polymers, is due to the preferential partitioning of mobile ions into the external solution (i.e., a Donnan mechanism). The concomitant increase in the osmotic pressure difference between the solution and mucus hydrogel results in this increase in compression.

CONCLUSIONS

There is considerable interest in understanding how diet impacts the composition and spatial structure of the gut microbiota and any concomitant effects that may impact the physical structure of the gut (e.g., mucus) and its physiology.^{4,14,15} However, few studies have focused on understanding the underlying physics behind how polymeric additives in food directly interact with gut structure and

physiology.⁶ Food science has traditionally focused more narrowly on aspects of food design such as the packaging, preservation, processing, and safety of food.^{9,57} However, research is showing that, at least in animal models, even at approved concentrations, some GRAS food additives are correlated with markers of disease (such as inflammation and obesity^{14,15}). Thus, it is important to improve our quantitative understanding of how these food additives interact with the host and modify gut physiology. In particular, there is a need to understand how food additives interact with mucus and the critical barrier in the colon that mediates host–microbe interactions and protects the host against physical damage.¹ Changes to the thickness and mesh size of the colonic mucus barrier have been associated with dramatic changes in host health.^{7,8,14}

In this work, we found that a polyelectrolyte, CMC, compresses mucus reversibly *in vivo*, in contrast to an emulsifier (Tween), which appeared to irreversibly disrupt mucus. We found that the amount of mucus compression induced by CMC increased as a function of the degree of polymer charge, which is a characteristic that has not been considered in the design of food products. Furthermore, we found that the increase in the amount of compression due to polymer charge is consistent with a Donnan mechanism. A simple, one-parameter model that combines the well-established theoretical frameworks of Flory–Huggins solution theory and Donnan partitioning was found to be sufficient to quantitatively capture the observed behavior. We have offered a potential explanation for the phenomenon observed in this work using the theoretical framework of Donnan partitioning; however, more comprehensive theoretical models need to be developed and tested to completely understand this mechanism and explicitly account for the possible penetration of polyelectrolytes into the mucus hydrogel.

Our work so far has not considered how fluid flow, possible rheological effects such as viscous relaxation of mucus on longer timescales,^{49,58} and possible anisotropy in the structure of the colonic mucus hydrogel² affect polymer-induced compression. Additionally, another factor *in vivo* is the regulation of isotonicity between the gut lumen and epithelium by the active transport of water and salts.⁵⁹ It is unclear how much this last factor would impact the observed phenomenon for two reasons: (i) small changes in the flux of water and salts will affect the base osmotic pressure (i.e., the osmotic pressure both inside the hydrogel and in the lumen) but not the difference in osmotic pressure inside and outside the hydrogel and (ii) our experiments and calculations suggest that the described Donnan effects disappear at tenfold physiological ionic strength, which is unlikely to occur *in vivo*. Finally, in our previous work, we found that the extent of mucus compression generally increased with the molecular weight of the polymer,⁶ but we have yet to consider if this relationship is further complicated by the polymer charge. All of these effects will be important areas to investigate in future work to understand how different polymers compress mucus *in vivo*.

The system we have considered in this work is an example of a class of systems consisting of a polyelectrolyte solution directly interacting with a biological, polyelectrolyte network. Such systems can be found throughout nature; other examples include biofilms in contact with extracellular DNA,⁶⁰ medical hydrogels in contact with gut polymers,⁶¹ ECM in contact with interstitial fluid,⁶² and hyaluronic acid–lubricin networks (which lubricate our joints) in contact with synovial fluid.⁶³

Our work begins to unravel this physics in the context of polyelectrolyte-induced mucus compression, which could lead to new, safer design of food products that do not alter the structure of colonic mucus.

■ ASSOCIATED CONTENT

Supporting Information

The Supporting Information is available free of charge on the ACS Publications website at DOI: [10.1021/acs.biomac.9b00442](https://doi.org/10.1021/acs.biomac.9b00442).

Derivation of the ionic contribution to osmotic pressure due to Donnan partitioning, estimation of the compression modulus for the colonic mucus hydrogel, figure depicting image processing, *ex vivo* compression reversibility data, gel permeation chromatography measurements of charged and uncharged polymers, and comparison of polymer and ionic contributions to the osmotic pressure (PDF)

Code to perform curve fitting in Figure 3B (ZIP)

■ AUTHOR INFORMATION

Corresponding Author

*E-mail: rustem.admin@caltech.edu. Tel: +1 626 395 2333. Fax: +1 626 568 8743.

ORCID

Asher Preska Steinberg: 0000-0002-8694-7224

Zhen-Gang Wang: 0000-0002-3361-6114

Rustem F. Ismagilov: 0000-0002-3680-4399

Author Contributions

A.P.S. and R.F.I. designed the research; A.P.S. performed the research; A.P.S. analyzed the data. Z.-G.W. guided the theoretical analysis. All authors wrote the paper.

Funding

Army Research Office (ARO) no. W911NF-17-1-0402; Jacobs Institute for Molecular Engineering for Medicine; Center for Environmental Microbial Interactions (CEMI); NSF Graduate Research Fellowship DGE-144469; Caldwell CEMI Graduate Fellowship.

Notes

The authors declare the following competing financial interest(s): The technology described in this publication is the subject of a patent application filed by Caltech.

■ ACKNOWLEDGMENTS

This work was supported in part by Army Research Office (ARO) Multidisciplinary University Research Initiative (MURI) contract no. W911NF-17-1-0402, the Jacobs Institute for Molecular Engineering for Medicine, the Center for Environmental Microbial Interactions (CEMI), an NSF Graduate Research Fellowship DGE-144469 (to A.P.S.), and a Caldwell CEMI Graduate Fellowship (to A.P.S.). We acknowledge Michael Porter for useful discussion and providing feedback on the manuscript; Andres Collazo and Caltech's Beckman Institute Biological Imaging Facility, the Caltech Office of Laboratory Animal Resources, and the Caltech veterinary technicians for technical support; Justin Rolando for providing microparticles; and Natasha Shelby for contributions to writing and editing this manuscript.

REFERENCES

- (1) Johansson, M. E. V.; Larsson, J. M. H.; Hansson, G. C. The Two Mucus Layers of Colon Are Organized by the MUC2 Mucin, Whereas the Outer Layer Is a Legislator of Host-Microbial Interactions. *Proc. Natl. Acad. Sci. U. S. A.* **2011**, *108*, 4659–4665.
- (2) Ambort, D.; Johansson, M. E. V.; Gustafsson, J. K.; Nilsson, H. E.; Ermund, A.; Johansson, B. R.; Koeck, P. J. B.; Hebert, H.; Hansson, G. C. Calcium and PH-Dependent Packing and Release of the Gel-Forming MUC2 Mucin. *Proc. Natl. Acad. Sci. U. S. A.* **2012**, *109*, 5645–5650.
- (3) Verdugo, P. Supramolecular Dynamics of Mucus. *Cold Spring Harbor Perspect. Med.* **2012**, *2*, a009597.
- (4) Desai, M. S.; Seekatz, A. M.; Koropatkin, N. M.; Kamada, N.; Hickey, C. A.; Wolter, M.; Pudlo, N. A.; Kitamoto, S.; Terrapon, N.; Muller, A.; Young, V. B.; Henrissat, B.; Wilmes, P.; Stappenbeck, T. S.; Núñez, G.; Martens, E. C. A Dietary Fiber-Deprived Gut Microbiota Degrades the Colonic Mucus Barrier and Enhances Pathogen Susceptibility. *Cell* **2016**, *167*, 1339–1353.e21.
- (5) Johansson, M. E. V.; Jakobsson, H. E.; Holmén-Larsson, J.; Schütte, A.; Ermund, A.; Rodríguez-Piñero, A. M.; Arike, L.; Wising, C.; Svensson, F.; Bäckhed, F.; Hansson, G. C. Normalization of Host Intestinal Mucus Layers Requires Long-Term Microbial Colonization. *Cell Host Microbe* **2015**, *582*–592.
- (6) Datta, S. S.; Preska Steinberg, A.; Ismagilov, R. F. Polymers in the Gut Compress the Colonic Mucus Hydrogel. *Proc. Natl. Acad. Sci. U. S. A.* **2016**, *113*, 7041–7046.
- (7) Johansson, M. E. V.; Gustafsson, J. K.; Holmén-Larsson, J.; Jabbar, K. S.; Xia, L.; Xu, H.; Ghishan, F. K.; Carvalho, F. A.; Gewirtz, A. T.; Sjövall, H.; Hansson, G. C. Bacteria Penetrate the Normally Impenetrable Inner Colon Mucus Layer in Both Murine Colitis Models and Patients with Ulcerative Colitis. *Gut* **2013**, *63*, 281–291.
- (8) Bergstrom, K. S. B.; Kissoon-Singh, V.; Gibson, D. L.; Ma, C.; Montero, M.; Sham, H. P.; Ryz, N.; Huang, T.; Velcich, A.; Finlay, B. B.; Chadee, K.; Vallance, B. A. Muc2 Protects against Lethal Infectious Colitis by Disassociating Pathogenic and Commensal Bacteria from the Colonic Mucosa. *PLoS Pathog.* **2010**, *6*, No. e1000902.
- (9) Goff, H. D.; Hartel, R. W. *Ice Cream*; Springer US, 2013.
- (10) Saha, D.; Bhattacharya, S. Hydrocolloids as Thickening and Gelling Agents in Food: A Critical Review. *J. Food Sci. Technol.* **2010**, *47*, 587–597.
- (11) FDA. CFR - Code of Federal Regulations Title 21. In *Current good manufacturing practice for finished pharmaceuticals Part 211*; U.S. Food and Drug Administration: 2018.
- (12) Hollabaugh, C. B.; Burt, L. H.; Walsh, A. P. Carboxymethylcellulose. Uses and Applications. *Ind. Eng. Chem.* **1945**, *37*, 943–947.
- (13) Leskauskaitė, D.; Jasutiene, I.; Kersiene, M.; Malinauskaitė, E.; Matusevicius, P. The Effect of Carboxymethyl Cellulose on the Stability of Emulsions Stabilized by Whey Proteins under Digestion in Vitro and in Vivo. *World Acad. Sci. Eng. Technol. Int. J. Biol. Biomol. Agric. Food Biotechnol. Eng.* **2013**, *7*, 51–56.
- (14) Chassaing, B.; Koren, O.; Goodrich, J. K.; Poole, A. C.; Srinivasan, S.; Ley, R. E.; Gewirtz, A. T. Dietary Emulsifiers Impact the Mouse Gut Microbiota Promoting Colitis and Metabolic Syndrome. *Nature* **2015**, *519*, 92–96.
- (15) Chassaing, B.; Van De Wiele, T.; De Bodt, J.; Marzorati, M.; Gewirtz, A. T. Dietary Emulsifiers Directly Alter Human Microbiota Composition and Gene Expression Ex Vivo Potentiating Intestinal Inflammation. *Gut* **2017**, *66*, 1414–1427.
- (16) Lock, J. Y.; Carlson, T. L.; Wang, C.-M.; Chen, A.; Carrier, R. L. Acute Exposure to Commonly Ingested Emulsifiers Alters Intestinal Mucus Structure and Transport Properties. *Sci. Rep.* **2018**, *8*, 10008.
- (17) Dobrynin, A.; Rubinstein, M. Theory of Polyelectrolytes in Solutions and at Surfaces. *Prog. Polym. Sci.* **2005**, *30*, 1049–1118.
- (18) Rubinstein, M.; Papoian, G. A. Polyelectrolytes in Biology and Soft Matter. *Soft Matter* **2012**, *8*, 9265.
- (19) Flory, P. J. *Principles of Polymer Chemistry*; Cornell University Press: Ithaca, New York, 1953.
- (20) Kudaibergenov, S. E.; Nuraje, N.; Khutoryanskiy, V. V. Amphoteric Nano-, Micro-, and Macrogels, Membranes, and Thin Films. *Soft Matter* **2012**, *8*, 9302–9321.
- (21) Priftis, D.; Tirrell, M. Phase Behaviour and Complex Coacervation of Aqueous Polypeptide Solutions. *Soft Matter* **2012**, *8*, 9396–9405.
- (22) De Kruijff, C. G.; Weinbreck, F.; De Vries, R. Complex Coacervation of Proteins and Anionic Polysaccharides. *Curr. Opin. Colloid Interface Sci.* **2004**, *9*, 340–349.
- (23) Schiessel, H.; Correa-Rodríguez, M. D.; Rudiuk, S.; Baigl, D.; Yoshikawa, K. Theory of DNA-Cationic Micelle Complexation. *Soft Matter* **2012**, *8*, 9406–9411.
- (24) Sennato, S.; Truzzolillo, D.; Bordini, F. Aggregation and Stability of Polyelectrolyte-Decorated Liposome Complexes in Water-Salt Media. *Soft Matter* **2012**, *8*, 9384–9395.
- (25) Kiefer, J.; Naser, M.; Kamel, A.; Carnali, J. Osmotic Deswelling of Microgels by Linear Polyelectrolytes. *Colloid Polym. Sci.* **1993**, *271*, 253–261.
- (26) Elderman, M.; Sovran, B.; Hugenholtz, F.; Graversen, K.; Huijskes, M.; Houtsma, E.; Belzer, C.; Boekschoten, M.; De Vos, P.; Dekker, J.; Wells, J.; Faas, M. The Effect of Age on the Intestinal Mucus Thickness, Microbiota Composition and Immunity in Relation to Sex in Mice. *PLoS One* **2017**, *12*, 1–22.
- (27) Sovran, B.; Hugenholtz, F.; Elderman, M.; Van Beek, A. A.; Graversen, K.; Huijskes, M.; Boekschoten, M. V.; Savelkoul, H. F. J.; De Vos, P.; Dekker, J.; Wells, J. M. Age-Associated Impairment of the Mucus Barrier Function Is Associated with Profound Changes in Microbiota and Immunity. *Sci. Rep.* **2019**, *9*, 1–13.
- (28) Leary, S.; Underwood, W.; Anthony, R.; Cartner, S. AVMA Guidelines for the Euthanasia of Animals: 2013 Edition. <https://www.avma.org/kb/policies/documents/euthanasia.pdf> (accessed Jun 11, 2018).
- (29) Preska Steinberg, A.; Datta, S. S.; Naragon, T.; Rolando, J. C.; Bogatyrev, S. R.; Ismagilov, R. F. High-Molecular-Weight Polymers from Dietary Fiber Drive Aggregation of Particulates in the Murine Small Intestine. *Elife* **2019**, *8*, No. e40387.
- (30) Hoogendam, C. W.; De Keizer, A.; Cohen Stuart, M. A.; Bijsterbosch, B. H.; Smit, J. A. M.; Van Dijk, J. A. P. P.; Van Der Horst, P. M.; Batelaan, J. G. Persistence Length of Carboxymethyl Cellulose as Evaluated from Size Exclusion Chromatography and Potentiometric Titrations. *Macromolecules* **1998**, *31*, 6297–6309.
- (31) Sjöholm, E. Size Exclusion Chromatography of Cellulose and Cellulose Derivatives. In *Handbook of Size Exclusion Chromatography and Related Techniques*; Marcel Dekker: 2004, 331–352.
- (32) Gustafsson, J. K.; Ermund, A.; Johansson, M. E. V.; Schütte, A.; Hansson, G. C.; Sjövall, H. An Ex Vivo Method for Studying Mucus Formation, Properties, and Thickness in Human Colonic Biopsies and Mouse Small and Large Intestinal Explants. *Am. J. Physiol. Gastrointest. Liver Physiol.* **2012**, *302*, G430–8.
- (33) Wang, Y.-Y.; Lai, S. K.; Suk, J. S.; Pace, A.; Cone, R.; Hanes, J. Addressing the PEG Mucoadhesivity Paradox to Engineer Nanoparticles That “Slip” through the Human Mucus Barrier. *Angew. Chem., Int. Ed.* **2008**, *47*, 9726–9729.
- (34) Viennois, E.; Merlin, D.; Gewirtz, A. T.; Chassaing, B. Dietary Emulsifier-Induced Low-Grade Inflammation Promotes Colon Carcinogenesis. *Cancer Res.* **2017**, *77*, 27–40.
- (35) Button, B.; Cai, L.-H.; Ehre, C.; Kesimer, M.; Hill, D. B.; Sheehan, J. K.; Boucher, R. C.; Rubinstein, M. A Periciliary Brush Promotes the Lung Health by Separating the Mucus Layer from Airway Epithelia. *Science* **2012**, *337*, 937–941.
- (36) Sierra-Martin, B.; Liator-Santos, J. J.; Fernandez-Barbero, A.; Nguyen, T. T.; Fernandez-Nieves, A. Swelling Thermodynamics of Microgel Particles. In *Microgel Suspensions*; Fernandez-Nieves, A., Wyss, H. M., Mattsson, J., Weitz, D. A., Eds.; Wiley-VCH: Weinheim, 2011; pp 71–116.

- (37) Carrillo, J.-M.; Dobrynin, A. Salt Effect on Osmotic Pressure of Polyelectrolyte Solutions: Simulation Study. *Polymer* **2014**, *6*, 1897–1913.
- (38) Peppas, N. A.; Khare, A. R. Preparation, Structure and Diffusional Behavior of Hydrogels in Controlled Release. *Adv. Drug Delivery Rev.* **1993**, *11*, 1–35.
- (39) Momii, T.; Nose, T. Concentration-Dependent Collapse of Polymer Gels in Solution of Incompatible Polymers. *Macromolecules* **1989**, *22*, 1384–1389.
- (40) Ito, T.; Yamazaki, M.; Ohnishi, S. Poly(Ethylene Glycol)-Induced Shrinkage of Sephadex Gel. A Model System for Quantitative Analysis of Osmoelastic Coupling. *Biophys. J.* **1989**, *56*, 707–711.
- (41) Adachi, K.; Nakamoto, T.; Kotaka, T. Swelling Equilibrium of Solution Cross-Linked Polybutadiene Networks in Polyisoprene Solutions. *Macromolecules* **1989**, *22*, 3106–3111.
- (42) Saunders, B. R.; Vincent, B. Thermal and Osmotic Deswelling of Poly(NIPAM) Microgel Particles. *J. Chem. Soc., Faraday Trans.* **1996**, *92*, 3385.
- (43) Ishida, T.; Akagi, M.; Sugimoto, H.; Iwai, Y.; Arai, Y. Swelling Behaviors of Poly (N-Isopropylacrylamide) Gel in Poly (Ethylene Glycol)-Water Mixtures. *Macromolecules* **1993**, *26*, 7361–7362.
- (44) Saunders, B. R.; Crowther, H. M.; Vincent, B. Poly[(Methyl Methacrylate)-Co-(Methacrylic Acid)] Microgel Particles: Swelling Control Using PH, Cononsolvency, and Osmotic Deswelling. *Macromolecules* **1997**, *30*, 482–487.
- (45) Kayaman, N.; Okay, O.; Baysal, B. M. Phase Transition of Polyacrylamide Gels in PEG Solutions. *Polym. Gels Networks* **1997**, *5*, 167–184.
- (46) Overbeek, J. T. G. The Donnan Equilibrium. *Prog. Biophys. Biophys. Chem.* **1956**, *6*, 58–64.
- (47) Li, L.; Lieleg, O.; Jang, S.; Ribbeck, K.; Han, J. A Microfluidic in Vitro System for the Quantitative Study of the Stomach Mucus Barrier Function. *Lab Chip* **2012**, *12*, 4071.
- (48) Perez-Vilar, J. Mucin Granule Intraluminal Organization. *Am. J. Respir. Cell Mol. Biol.* **2007**, *36*, 183–190.
- (49) Lai, S. K.; Wang, Y.-Y.; Wirtz, D.; Hanes, J. Micro- and Macrorheology of Mucus. *Adv Drug Deliv Rev* **2009**, *61*, 86–100.
- (50) Georgiades, P.; Pudney, P. D. A.; Thornton, D. J.; Waigh, T. A. Particle Tracking Microrheology of Purified Gastrointestinal Mucins. *Biopolymers* **2014**, *101*, 366–377.
- (51) Tanford, C. *Physical Chemistry of Macromolecules*; Wiley: New York, 1961.
- (52) Rubinstein, M.; Colby, R. H. *Polymer Physics*; OUP Oxford: New York, 2003.
- (53) Kong, H. J.; Lee, K. Y.; Mooney, D. J. Decoupling the Dependence of Rheological/Mechanical Properties of Hydrogels from Solids Concentration. *Polymer* **2002**, *43*, 6239–6246.
- (54) Boral, S.; Saxena, A.; Bohidar, H. B. Syneresis in Agar Hydrogels. *Int. J. Biol. Macromol.* **2010**, *46*, 232–236.
- (55) Skouri, R.; Schosseler, F.; Munch, J. P.; Candau, S. J. Swelling and Elastic Properties of Polyelectrolyte Gels. *Macromolecules* **1995**, *28*, 197–210.
- (56) Muniz, E. C.; Geuskens, G. Compressive Elastic Modulus of Polyacrylamide Hydrogels and Semi-IPNs with Poly(N-Isopropylacrylamide). *Macromolecules* **2001**, *34*, 4480–4484.
- (57) Potter, N.; Hotchkiss, J. *Food Science*; 5th ed.; Springer Science & Business Media: New York, 1998.
- (58) Sellers, L. A.; Allen, A.; Morris, E. R.; Ross-Murphy, S. B. The Rheology of Pig Small Intestinal and Colonic Mucus: Weakening of Gel Structure by Non-Mucin Components. *Biochim. Biophys. Acta, Gen. Subj.* **1991**, *1115*, 174–179.
- (59) Keely, S. J.; Montrose, M. H.; Barrett, K. E. *Electrolyte Secretion and Absorption: Small Intestine and Colon*; John Wiley & Sons, Inc.: 2009, Vol. 1.
- (60) Flemming, H.-C.; Wingender, J. The Biofilm Matrix. *Nat. Rev. Microbiol.* **2003**, *19*, 139–150.
- (61) Sharpe, L. A.; Daily, A. M.; Horava, S. D.; Peppas, N. A. Therapeutic Applications of Hydrogels in Oral Drug Delivery. *Expert Opin. Drug Delivery* **2014**, *11*, 901–915.
- (62) Wiig, H.; Swartz, M. A. Interstitial Fluid and Lymph Formation and Transport: Physiological Regulation and Roles in Inflammation and Cancer. *Physiol. Rev.* **2012**, *92*, 1005–1060.
- (63) Greene, G. W.; Banquy, X.; Lee, D. W.; Lowrey, D. D.; Yu, J.; Israelachvili, J. N. Adaptive Mechanically Controlled Lubrication Mechanism Found in Articular Joints. *Proc. Natl. Acad. Sci. U. S. A.* **2011**, *108*, S255–S259.